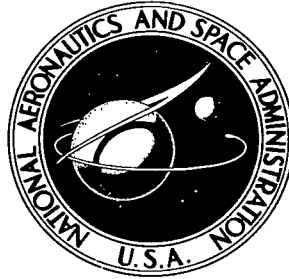


NASA TECHNICAL NOTE



NASA TN D-8369 *cl*

NASA TN D-8369

LOAN COPY: RET  
APWL TECHNICAL  
KIRTLAND AFB,



A FOREBODY DESIGN TECHNIQUE FOR HIGHLY  
INTEGRATED BOTTOM-MOUNTED SCRAMJETS  
WITH APPLICATION TO A HYPERSONIC  
RESEARCH AIRPLANE

*C. L. W. Edwards*

*Langley Research Center  
Hampton, Va. 23665*



NATIONAL AERONAUTICS AND SPACE ADMINISTRATION • WASHINGTON, D. C. • DECEMBER 1976



0134105

1. Report No. NASA TN D-8369		2. Government Accession No.	
4. Title and Subtitle A FOREBODY DESIGN TECHNIQUE FOR HIGHLY INTEGRATED BOTTOM-MOUNTED SCRAMJETS WITH APPLICATION TO A HYPERSONIC RESEARCH AIRPLANE		5. Report Date December 1976	
7. Author(s) C. L. W. Edwards		6. Performing Organization Code	
9. Performing Organization Name and Address NASA Langley Research Center Hampton, VA 23665		8. Performing Organization Report No. L-11265	
12. Sponsoring Agency Name and Address National Aeronautics and Space Administration Washington, DC 20546		10. Work Unit No. 505-11-31-02	
15. Supplementary Notes		11. Contract or Grant No.	
16. Abstract <p>A rapid and simple inviscid technique for designing forebodies which produce uniformly precompressed flows at the inlet entrance for bottom-mounted scramjets has been developed so that geometric constraints resulting from design trade-offs can be effectively evaluated. The flow fields resulting from several forebody designs generated in support of a conceptual design for a hypersonic research airplane have been analyzed in detail. Three-dimensional characteristics calculations were used to verify the uniform flow conditions. For the designs analyzed, uniform flow was maintained over a wide range of flight conditions (Mach numbers from 4 to 10; angles of attack of 6° and 10°) corresponding to the scramjet operation flight envelope of the research airplane.</p>		13. Type of Report and Period Covered Technical Note	
17. Key Words (Suggested by Author(s)) Forebody design Uniform flow Engine-airframe integration Inlet flows Precompression		14. Sponsoring Agency Code	
18. Distribution Statement Unclassified - Unlimited		Subject Category 05	
19. Security Classif. (of this report) Unclassified	20. Security Classif. (of this page) Unclassified	21. No. of Pages 29	22. Price* \$3.75

A FOREBODY DESIGN TECHNIQUE FOR HIGHLY INTEGRATED BOTTOM-MOUNTED  
SCRAMJETS WITH APPLICATION TO A HYPERSONIC RESEARCH AIRPLANE

C. L. W. Edwards  
Langley Research Center

SUMMARY

The efficiency of future hypersonic airbreathing aircraft depends to a great extent on the maximum integration of the propulsion system with the vehicle airframe. A rapid and simple inviscid technique for designing forebodies which produce uniformly precompressed flows at the inlet entrance for bottom-mounted scramjets has been developed so that geometric constraints resulting from design trade-offs can be effectively evaluated. The flow fields resulting from several forebody designs generated in support of a conceptual design for a hypersonic research airplane have been analyzed in detail. Three-dimensional characteristics calculations were used to verify uniform flow conditions. For the designs analyzed, uniform flow is maintained over a wide range of flight conditions corresponding to the scramjet operation flight envelope of the research airplane.

INTRODUCTION

A large spectrum of promising future military and civil applications of hydrogen-fueled airbreathing aircraft for high supersonic and hypersonic flight has been well documented in the literature. (See refs. 1 to 5.) A common feature of these aircraft is the necessity to integrate the propulsion system with the vehicle airframe carefully to obtain optimum overall performance. As shown in figure 1, the size of the propulsion system relative to aircraft size increases rapidly with increasing flight Mach number, and the forces (discussed in ref. 6) generated by the propulsion system become large when compared with aerodynamic forces. Mutual interactions between these large forces are advantageous when the propulsion system is properly integrated with the vehicle airframe. Thus, the engine-airframe integration process represents a major design opportunity to maximize the performance of hypersonic airbreathing vehicles.

The highly integrated aircraft concepts depicted in figure 1 are attractive because they provide both maximum inlet capture area and maximum nozzle expansion area while maintaining minimum cowl drag. However, full advantage of this arrangement can be taken only when the vehicle propulsion system is properly integrated early in the design process. Some interactive constraints which must be considered in the design of highly integrated hypersonic systems are shown in figure 2. The size and number of the engines must be sufficient to meet mission requirements. The scramjet inlet must be located within the forebody compression field to obtain maximum performance. An effective precompression tends to reduce the physical dimensions of the inlet. This reduction in turn tends to reduce engine weight and cowl drag. If the precompressed flow at the inlet face

can also be made uniform, the increased complexity in inlet design required for efficient operation in widely varying flows can also be alleviated. However, the available shock-layer capture area decreases with Mach number so that the inlet must capture most of the flow between the body and the bow shock across the entire fuselage span. The engine size and the flow-field requirements are not the only considerations necessary for a good forebody design. Aerodynamic, structural, and internal volume requirements are other constraints which must be incorporated early in the design process to achieve an optimum configuration.

The scramjet nozzle design is primarily governed by thrust and stability requirements. Thus, the location of the scramjet, orientation of the thrust vector, and the resulting trim penalties must be examined across the entire flight envelope (ref. 6). The strong interaction between the nozzle exhaust and the nonuniform flows surrounding the vehicle afterbody and external cowl must also be accounted for in the evaluation of nozzle performance.

It is apparent, therefore, that one key to optimum vehicle performance is a systematic procedure for effectively assessing the interactive constraints early in the design, if any realistic beneficial coupling between the engine and airframe is to be achieved. A significant research effort is being made at Langley Research Center to examine, to develop, and to validate the technology necessary to perform such assessments during the design process on a routine basis. The engine-nozzle-vehicle interactions and design methodology are presented in reference 6. The primary objectives of this paper are to describe recent progress in forebody design methodology, to present some results from a vehicle design study, and to indicate some areas of research which could enhance overall design capability.

#### SYMBOLS

$A$	forebody cross-sectional area
$A_c$	inlet capture area
$D$	axial design length of constant impact-angle surface
$h$	inlet height
$\hat{i}, \hat{j}, \hat{k}$	unit vector components in x-, y-, and z-directions, respectively
$M$	Mach number
$\vec{n}$	outward unit normal surface vector
$n_x, n_y, n_z$	directional cosines of outward unit normal surface vector
$P, Q, R, S, T, SG$	lofting-curve coefficients for forebody geometry
$p$	static pressure
$r$	radius of equivalent circular forebody cross section

$S_{ref}$	vehicle reference area
$\vec{S}$	surface tangent vector in Newtonian stream direction
$V$	velocity
$\frac{V_x}{ V }, \frac{V_y}{ V }, \frac{V_z}{ V }$	directional cosines of velocity vector
$\vec{V}$	velocity vector
$\vec{v}$	unit vector in velocity direction
$X, Y, Z$	forebody reference coordinates
$x, y, z$	distance along the axes
$\alpha$	angle of attack referenced to lower surface center line of forebody at inlet entrance
$\delta$	Newtonian impact angle
$\theta_0$	lower forebody center-line deflection angle
$\mu$	Mach angle, $\sin^{-1} (1/M)$
$\rho$	density
$\frac{\rho V}{\rho_\infty V_\infty}$	local to free-stream mass flow ratio
$\phi$	forebody cross-section meridian angle
Subscripts:	
$I$	inlet
$l, m$	indices for lofting-line coefficients
$\infty$	free-stream conditions

### FOREBODY DESIGN PROCEDURE

The forebody design goals are indicated in figure 3. The key flow parameters and the region at the inlet entrance requiring uniform precompression are also shown. The cross-sectional area (located at the inlet face) in which the flow is to be tightly constrained is bounded by the vehicle surface and two functions of engine geometry: (1) the position of the outboard engine module and (2) the position of the cowl lip (or bow shock as the Mach number becomes large). This control area is represented by the crosshatched region in figure 3. An ideal and probably unattainable design would render the oncoming precompressed

flow parallel and uniform in the control area. This flow would also remain invariant with changes in Mach number and angle of attack. The practical goal for this study was to develop a straightforward design procedure which can be used effectively to minimize gradients in key flow parameters in the region of the inlet entrance over the vehicle flight envelope.

The parameters which directly influence inlet and engine performance are mass flow to be ingested, static pressure, local Mach number, and flow angularity. These parameters are sufficient to define the state of the flow and if they are uniform, it follows that the remaining flow variables are also uniform. The predominant parameter, and therefore a good approximate measure of forebody effectiveness, is the relative mass flow. A reduction in mass flow would cause a corresponding reduction in thrust available from a fixed size engine, and large gradients in mass flow would require complex fuel scheduling between engine modules to achieve maximum performance.

### Computational Techniques

Several numerical techniques can be used to calculate supersonic inviscid flows over three-dimensional geometries. (See refs. 7 to 10.) In principle, any of these techniques could be employed to derive a geometry which produces uniform flow at the inlet entrance. Either parametric studies of several geometries or an inverse approach using one of these techniques to solve for the appropriate geometric boundary directly could be employed. The parametric approach appears to be too restrictive and time consuming for the preliminary design process. The inverse technique can, in principle, be carried out by specifying the inlet station flow conditions and by performing an upwind numerical calculation (characteristics or finite difference) to solve for a geometry which maintains the specified flow. However, the resulting geometry could be very difficult to constrain so that required trade-offs could be performed on the basis of other multidisciplinary functions of merit which must be considered to achieve a realistic optimum. The complexity required for this procedure did not seem warranted for the preliminary design task since one of the basic study goals was to develop a straightforward and rapid preliminary design tool. Therefore, the approach taken in this study is a highly simplified analogy to the inverse technique where basic hypersonic flow relations are used in lieu of more exact numerical schemes to determine the appropriate forebody geometry.

### Design Method

At hypersonic speeds, Newtonian flow gives a good representation of the inviscid conditions on three-dimensional compression surfaces which do not produce strong crossflows or embedded shocks. Since the shock layer is thin, the surface conditions should also represent the conditions in the field if those surface conditions are uniform everywhere over the control area. In addition, the surface geodesics (defined in the classical sense as the shortest surface distance between two points) become streamlines when the surface pressure is constant. Therefore, the problem is one of creating a geometry from the Newtonian stream directions so that the Newtonian impact angle is constant (fig. 4).

The classic equation for the Newtonian impact angle  $\delta$  in terms of the velocity vector

$$\vec{V} = V_x \hat{i} + V_y \hat{j} + V_z \hat{k} \quad (1)$$

and the outward normal to the surface

$$\vec{n} = n_x \hat{i} + n_y \hat{j} + n_z \hat{k} \quad (2)$$

is

$$\sin \delta = -\left(\frac{n_x V_x}{|V|} + \frac{n_y V_y}{|V|} + \frac{n_z V_z}{|V|}\right) \quad (3)$$

If the velocity vector is a function of angle of attack  $\alpha$  only (no yaw), then a unit vector in the velocity direction can be defined by

$$\vec{v} = \cos \alpha \hat{j} + \sin \alpha \hat{k} \quad (4)$$

and the Newtonian impact angle becomes

$$\sin \delta = -(n_y \cos \alpha + n_z \sin \alpha) \quad (5)$$

By solving equation (5) for  $n_y$  and substituting into equation (2), the normal vector in terms of  $n_x$  and  $n_z$  becomes

$$\vec{n} = n_x \hat{i} - \left(\frac{n_z \sin \alpha + \sin \delta}{\cos \alpha}\right) \hat{j} + n_z \hat{k} \quad (6)$$

Then,  $n_x$  can be determined from the local cross-section curve of the vehicle by relating its slope to the surface normal

$$n_x = -n_z \tan \phi \quad (7)$$

where

$$\tan \phi = \frac{dz}{dx} \quad (8)$$

Substituting equation (7) into equation (6) produces

$$\vec{n} = -n_z \tan \phi \hat{i} - \left(\frac{n_z \sin \alpha + \sin \delta}{\cos \alpha}\right) \hat{j} + n_z \hat{k} \quad (9)$$

and since by definition

$$\vec{n} \cdot \vec{n} = n_x^2 + n_y^2 + n_z^2 = 1 \quad (10)$$

$n_z$  can be determined in terms of the vehicle angle of attack, Newtonian impact angle, and cross-sectional geometry from equations (9) and (10):

$$n_z = \frac{-\sin \delta \sin \alpha - \cos \alpha \sqrt{\cos^2 \delta + (\cos^2 \alpha - \sin^2 \delta) \tan^2 \phi}}{1 + \cos^2 \alpha \tan^2 \phi} \quad (11)$$

The relations for  $n_x$  and  $n_y$  in terms of the same parameters become

$$n_x = \frac{\left[ \sin \delta \sin \alpha + \cos \alpha \sqrt{\cos^2 \delta + (\cos^2 \alpha - \sin^2 \delta) \tan^2 \phi} \right] \tan \phi}{1 + \cos^2 \alpha \tan^2 \phi} \quad (12)$$

and

$$n_y = \frac{-\sin \delta \cos \alpha + \sin \alpha \sqrt{\cos^2 \delta + (\cos^2 \alpha - \sin^2 \delta) \tan^2 \phi} \cos^2 \phi}{\cos^2 \phi + \cos^2 \alpha \sin^2 \phi} \quad (13)$$

The geodesic directions are maintained coincident with the Newtonian stream direction  $\vec{S}$  which can be determined by taking successive vector products between the surface normal and the wind vector

$$\vec{S} = \vec{n} \times (\vec{n} \times \vec{v}) \quad (14)$$

as illustrated in the vector diagram of figure 4. Any number of geodesic directions can be determined along a given cross section and projected upstream some arbitrary distance  $\Delta y$ . The locus of these projected geodesics can then be used to define a new upstream cross section, and the process can be repeated until the desired surface is fully determined.

The preliminary design method illustrated here was developed for arbitrary forebody geometry; however, the numerical methods available to verify the flow fields are somewhat geometry restricted. Three-dimensional characteristics calculations made with the computer program of reference 7 were used in this study to verify the design technique. This characteristics program is limited to smooth continuous geometries with bielliptic cross sections. However, general variation in the longitudinal direction is allowed, as illustrated in figure 5, by defining the projections of three lofting lines in the vehicle coordinate planes with a series of segments using the general conic equation

$$\begin{pmatrix} x \\ z \end{pmatrix}_{\ell, m} = P_{\ell, m} Y + Q_{\ell, m} + (SG)_{\ell, m} \sqrt{R_{\ell, m} Y^2 + S_{\ell, m} Y + T_{\ell, m}} \quad (15)$$

where  $\ell$  denotes the segment and  $m$  denotes the six projections of the three lofting curves on the coordinate planes.

Constant impact angle is not necessary over the entire undersurface of the forebody since influence at the inlet station from upstream geometry is not generally felt past a point where a Mach wave from the body intersects the cowl lip. This distance is illustrated in figure 5 and is the upstream boundary for which the forebody must be closely tailored. Since the flow is not likely to be entirely uniform between body and bow shock, the largest free-stream Mach

number in the vehicle flight envelope is used to specify the upstream boundary to insure adequate design length  $D$  to develop uniform flow at the inlet face:

$$D = \frac{h}{\tan(\theta_o + \mu) - \tan \theta_o} \quad (16)$$

where  $\theta_o$  is determined by the center-line ( $\phi$ ) slope

$$\theta_o = \tan^{-1} \left( \frac{dz}{dy} \right)_{\phi} \quad (17)$$

and  $\mu$  is the free-stream Mach angle

$$\mu = \sin^{-1} \left( \frac{1}{M_{\infty}} \right) \quad (18)$$

The lower center-line geodesic is kept straight over the design length but is allowed to curve upstream of this point to meet aerodynamic and volumetric constraints. However, care must be taken to avoid rapid expansions in the forward portion since the Newtonian concept will not account for strong overexpansion which could alter the flow at the inlet entrance.

Uniform Newtonian impact angle need not be imposed over the entire under-surface span since the spanwise control boundary is initially defined by the width of the engines, where the engine width is determined from preliminary inlet capture requirements and the cowl or shock height. The surface geodesics define the spanwise boundary upstream of the inlet station (fig. 5). However, the overall forebody planform is unrestricted. The assumptions used to establish the boundaries over which the surface must be tailored are quite adequate for bottom-mounted engines, and variations of this technique could be expected to produce uniformly precompressed flows for side-mounted or displaced inlets. However, at lower Mach numbers (e.g.,  $M_{\infty} < 3$ ), a more sophisticated procedure such as linear theory may be required to determine the Mach lines which define the body surface and inlet cowl boundaries.

## RESULTS AND DISCUSSION

This forebody design method has been applied to a hypersonic research airplane design study, and the resulting flow fields were verified by calculations of the three-dimensional characteristics. The basic vehicle illustrated in figure 6 was designed to take advantage of several advanced and promising new concepts for high-performance airbreathing hypersonic aircraft. Fixed-geometry scramjets were fully integrated with the vehicle airframe where the forebody was used to precompress the inlet flow uniformly, and the entire afterbody was used as an exhaust nozzle. Structures, propulsion, aerodynamics, and systems requirements were considered in producing a vehicle capable of systematically flight testing several of the most promising advanced concepts for hypersonic flight (ref. 11). The payloads and overall flight capability of this vehicle are beyond the scope of this paper; however, several features which affect the forebody design are presented here. This vehicle was to be air launched and

rocket accelerated to at least Mach 4. Scramjet acceleration and cruise capability were required at all speeds between Mach 4 and Mach 10. The scramjet engine employed was a hydrogen-fueled fixed-geometry modular design currently under development at Langley Research Center (refs. 12 and 13). Identical modules were imposed as a ground rule in the research airplane design study to minimize the complexity and cost of the research scramjet propulsion system. The vehicle forebody geometry was tightly constrained by the large forward volume requirements in the payload bay to accommodate the hydrogen fuel tank and the size limitations imposed by the carrier vehicle (B-52).

Some of the potential performance payoffs which can be achieved through forebody design are illustrated through the key constraints and flow requirements imposed in this design study. The volume of the forebody is generally determined without considering the inlet flow conditions and is primarily a function of the internal system requirements, center-of-gravity control, and vehicle aerodynamics. A perspective of the volume requirements imposed in this study is indicated in figure 7, where the cross-sectional area and radius of an equivalent axisymmetric body for the design vehicle are presented as a function of distance from the nose. The distributions for a cone and an ogive cylinder are shown for comparison. The length of the cylinder on the ogive cylinder was determined from equation (16) using the initial cowl height and center-line pre-compression requirements for the research airplane concept. The cone which gives the closest approximation to the planform and profile limitations of the vehicle has a  $5^\circ$  half-angle. These three bodies form a boundary of potential axisymmetric forebody designs.

#### Mach 10 Forebody Flows

If the flow field about the three bounding forebodies (fig. 7) at flight conditions is assumed to correspond approximately to Mach 10 cruise, the flow at the inlet entrance is obviously not uniform (see fig. 8). The angle of attack of each body was determined so that the local angle between the lower center line and the wind vector was  $10^\circ$  at the inlet entrance. The local Mach number, pressure ratio, and relative mass flow are presented near the body surface and at a specified cowl height as a function of percent body semispan. These data were obtained from the three-dimensional characteristics program of reference 7. Each of these bodies exhibits a strong spanwise variation in each of the flow parameters, and except for the cone, there is a significant variation between body and cowl lip at each spanwise location.

The possible detrimental effect of such flows on engine performance can be readily seen by examining the variation in relative mass flow across the vehicle span. For the vehicle displayed in figure 6, the mass-flow requirements to meet mission goals were initially based on design center-line (surface plane of symmetry) values and engine installation across 80 percent of the body semispan. An examination of the average mass flow across the span of these three bodies, as illustrated in figure 8, indicates a 25-percent dropoff from the center-line design value to the most outboard position (80-percent semispan). A corresponding engine performance potential roughly 25 percent less than the initial design value is also indicated.

This parameter does not give an exact representation of performance potential because the shock standoff distance increases from the center line out across the span, and more inlet capture could be used if nonsimilar modules were employed. However, as stated earlier, use of identical engine modules was a ground rule for this study.

The forebody design procedure based on Newtonian impact angle was used to create a geometry within the forebody volume constraints of the research airplane. The spanwise area of interest included 80 percent of the semispan, and the upstream boundary was determined from Mach 10 cruise conditions. Maximum effective inlet capture becomes increasingly important with increasing Mach number; therefore, the bow shock was taken as the vertical boundary at the inlet face. The flow at the inlet face from this forebody design is superimposed (fig. 9) on the previous results for the axisymmetric equivalent to the research airplane forebody (based on cross-sectional area distribution). The cross-hatched regions denote the axisymmetric forebody results of figure 8(b). Both the spanwise and vertical variations in all parameters are markedly decreased; the most graphic improvement occurs, however, in the available mass flow across the 80-percent semispan of interest. The average center-line value of mass flow for the tailored forebody is increased by approximately 25 percent over that of the axisymmetric equivalent even though the local surface center-line inclination at the inlet entrance is  $10^\circ$  for both forebodies. The integrated average mass flow across 80 percent of the semispan of the tailored forebody is approximately 33.5 percent higher than that of the axisymmetric equivalent. The angle of attack of the axisymmetric equivalent could be increased until the average center-line values of mass flow were equal on the two forebodies; however, the integrated average mass flow on the tailored forebody would still be approximately 7 percent larger than the axisymmetric equivalent. This difference is amplified by the increased flow nonuniformity that is bound to occur on the axisymmetric forebody as the angle of attack is increased. These comparative advantages of tailored forebodies are significant; however, a more objective evaluation of the design technique can be made by analyzing inlet entrance flows in light of the forebody design goals listed in figure 3.

Several alternate designs were generated during this study, and additional flow parameters such as shock standoff distance and flow angularity were examined to assess their relationship to the forebody-inlet interaction. Three forebodies with variations in fineness ratio (volume) and cross-sectional shape are shown in figure 10. As stated earlier, the forebodies presented in this paper are constructed from bielliptic cross sections so that the flow fields could be verified with the calculations for the three-dimensional characteristics by using the method of reference 7. The major to minor axis ratios for the lower surfaces of forebodies 1, 2, and 3 are 7, 3.5, and 2, respectively. The spanwise control boundary for each of these bodies was at 80 percent of the body semispan. The design angle of attack was  $10^\circ$  relative to the lower surface center line, and the boundary height perpendicular to the surface was taken as the shock height at flight conditions of  $M_\infty = 10$  and  $\alpha = 10^\circ$ . The body listed as forebody 1 is the same forebody presented in figure 9. The flow conditions at the inlet face (control area) which are generated by these forebodies are shown in figure 11. The spanwise variations of each parameter are small, as are the variations from body to cowl lip (bow shock). The magnitudes of these variations are discussed more fully later in the paper. The main point illustrated

in figure 11 is the close similarity between these flows even though the fineness ratios and cross-sectional shapes are quite different (e.g., the average local cross-sectional curvature of forebody 3 is approximately twice that of forebody 1).

A more complete representation of the flow at the inlet face is illustrated by inlet station isograms in figures 12 to 14. These isograms clearly indicate the variations in pressure, local Mach number, flow sidewash angle, relative mass flow, and the shock standoff distances. The lateral bound of the control area is indicated in each figure by a dashed line normal to the surface. The maximum pressure deviation over the control area for all three bodies is less than 10 percent. The local values and gradients are similar for each of the three forebodies. The maximum local Mach number deviation is 5 percent or less. The predominant flow parameter is mass flow. The mass flow changes in distribution for these forebodies from a slightly vertically striated flow for forebody design 1 to a slightly spanwise striated flow for forebody design 3. The maximum spanwise deviation is less than 4 percent for each forebody. The maximum overall deviation in mass flow is 10 percent. This deviation occurs between body and shock for forebody 1.

The deviation in sidewash flow angle over the control area could affect inlet performance, and the maximum deviation of  $4.5^\circ$  occurs on forebody 3 as expected because of its increased cross-sectional curvature. However, the effect of this flow angularity can be reduced to acceptable levels without additional forebody tailoring because of the modular design of the scramjet. Five engine modules were used across the total span, and if each module is aligned with the average direction of the flow being captured, the maximum flow angularity experienced by any one module is less than  $\pm 1^\circ$ . However, a small external cowl drag penalty is incurred when the modules are canted inboard. Thus, the optimum orientation of the engine modules must be determined through trade-offs between cowl drag and inlet performance.

Maximum effective inlet capture is also a forebody design goal. For the integration concept in this study, maximum effective inlet capture occurs when the forebody bow shock coincides with the cowl lip. Uniformity of shock standoff distance is the primary criterion of merit in achieving this goal within the identical engine module constraint. For these bodies, the shock standoff distance decreases slightly across the body semispan, and the minimum height occurs at the outboard control area boundary. All three forebodies provided approximately 90-percent effective capture of the available precompressed flow when constrained to the largest constant height inlets that could be accommodated between the body and bow shock.

For the three forebody designs illustrated in figures 12 to 14, the shock standoff distance at the design Mach number and design angle of attack was approximately equal to one-half the body semispan. Therefore, forebody 1 has higher drag because of its lower fineness ratio, and the final choice is a trade-off between aerodynamic and inlet capture efficiencies. In this study, the volume constraint tended to drive the optimum choice toward forebody 1. The nearly linear variation of shock standoff distance with forebody semispan for these bodies also allows rapid estimates of inlet capture efficiency within moderate

changes in longitudinal engine location, a key parameter in nozzle integration (ref. 6).

### Off-Design Forebody Flows

The inlet entrance flow at off-design flight conditions resulting from tailored forebodies also plays an important role in the overall measure of forebody effectiveness since the vehicle must perform efficiently at Mach numbers and angles of attack other than those encountered at cruise. The scramjet acceleration portions of the flight envelope of this vehicle resulted in approximate forebody angles of attack of  $6^\circ$  across the Mach number range. The primary flow parameters (local Mach number, pressure, and relative mass flow for the three forebodies) are presented in figure 15 as functions of percent body semispan for Mach 10 accelerations.

Again, the relative mass flow is a key parameter in determining forebody effectiveness. The average mass flow for each forebody design was reduced because of the lower angle of attack; therefore, the real criteria of merit are the vertical and spanwise mass-flow variations across the inlet face. A slight positive spanwise gradient occurs at Mach 10 at the  $6^\circ$  acceleration angle of attack. This is most noticeable in the surface values for forebody 1; however, the maximum spanwise variation for each forebody occurs near the 80-percent semispan location and deviates less than 6 percent from the center-line value. These gradients are slightly positive in contrast to the large negative gradients shown for the axisymmetric bodies in figure 8. The slight positive gradients could be beneficial if an increase in fuel scheduling complexity were acceptable. The vertical gradients in mass flow are almost identical with those shown in figure 11 for the cruise conditions and are within the design goals.

The variations in inlet flow conditions with flight Mach number are shown for forebody 1 in figure 16. The same three flow parameters are again presented as the basic measure of merit for Mach numbers 4, 6, and 8 at acceleration angle of attack. At the lower Mach number, a negative spanwise gradient in both pressure and relative mass flow occurs slightly inboard of the 80-percent semispan control boundary. However, the spanwise gradients shown in figure 16 from Mach 4 to Mach 8 are less than the vertical gradient in mass flow for forebody 1 at cruise design conditions. The magnitudes of these off-design variations are within the initial forebody design goals.

### AREAS FOR FUTURE STUDY

The results of this study represent a first step in developing the technological base necessary to integrate scramjets with the vehicle airframe efficiently by identifying some major trends resulting from forebody-inlet-airframe interactions. However, much remains to be done before optimum integration can realistically be achieved. Some forebody-inlet items which are amenable to state-of-the-art analytic techniques currently under investigation are listed as follows:

(1) The effects of boundary-layer displacement and other viscous effects must be included in the forebody tailoring scheme.

(2) The effect of vehicle yaw on forebody flow fields must be assessed.

(3) Forebodies employing hard chines at maximum span should permit the highest percent span utilization and should be included in analytic capability.

(4) At lower Mach numbers ( $M_\infty < 3$ ), more exact techniques for determining the forebody influence boundaries must be applied for side-mounted inlets or for inlets which are significantly displaced from the vehicle surface.

#### CONCLUDING REMARKS

The geometric shape of forebodies on highly integrated hypersonic vehicles has a significant effect on the overall vehicle performance. When the flow at the inlet entrance has been uniformly precompressed, the engine size, weight, and drag can be more easily minimized. In addition, uniform flow has a beneficial effect on the required complexities in inlet design and fuel scheduling between engine modules.

A forebody design procedure has been developed to generate surfaces which produce nearly uniform flows at the entrance of bottom-mounted inlets. The procedure has been verified in a vehicle design study where several forebodies were generated. These forebodies exhibited minimum variations in key flow parameters across both the vehicle span and the shock layer. The bow shock standoff distance was also rendered nearly uniform so that at hypersonic cruise conditions a near-maximum effective inlet capture schedule can be achieved. Flow angularities were examined, and although they were not nulled, they were found to be of acceptable levels (less than  $\pm 1^\circ$  across any single engine module employed in the design study). The basic nature of the forebody flow is maintained across the normal scramjet portion of the design vehicle flight envelope which included a Mach number range from 4 to 10 and angles of attack of  $6^\circ$  and  $10^\circ$ .

These studies indicate that good inlet flow can be achieved by tailoring only the portion of the vehicle surface which has direct influence upon the inlet capture area. Therefore, reasonable geometries can be generated to meet constraints which are imposed by other disciplines such as aerodynamics, structures, and internal systems.

Langley Research Center  
National Aeronautics and Space Administration  
Hampton, VA 23665  
December 6, 1976

## REFERENCES

1. Becker, John V.; and Kirkham, Frank S.: Hypersonic Transports. Vehicle Technology for Civil Aviation - The Seventies and Beyond, NASA SP-292, 1971, pp. 429-445.
2. Nagel, A. L.; and Becker, J. V.: Key Technology for Airbreathing Hypersonic Aircraft. AIAA Paper No. 73-58, Jan. 1973.
3. Becker, John V.: Prospects for Actively Cooled Hypersonic Transports. Astronaut. & Aeronaut., vol. 9, no. 8, Aug. 1971, pp. 32-39.
4. Small, W. J.; Fetterman, D. E.; and Bonner, T. F., Jr.: Alternate Fuels for Transportation. Mech. Eng., vol. 96, no. 5, May 1974, pp. 18-24.
5. Gregory, T. J.; Williams, L. J.; and Wilcox, D. E.: Airbreathing Launch Vehicle for Earth Orbit Shuttle - Performance and Operation. J. Aircraft, vol. 8, no. 9, Sept. 1971, pp. 724-731.
6. Small, William J.; Weidner, John P.; and Johnston, P. J.: Scramjet Nozzle Design and Analysis as Applied to a Highly Integrated Hypersonic Research Airplane. NASA TN D-8334, 1976.
7. Chu, C. W.; and Powers, S. A.: The Calculation of Three-Dimensional Supersonic Flows Around Spherically-Capped Smooth Bodies and Wings. AFFDL-TR-72-91, Vols. I and II, U.S. Air Force, Sept. 1972.
8. Gunness, R. C., Jr.; Knight, C. J.; and D'Sylva, E.: Flow Field Analysis of Aircraft Configurations Using a Numerical Solution to the Three-Dimensional Unified Supersonic/Hypersonic Small-Disturbance Equations. Part I. NASA CR-1926, 1972.
9. Rakich, John V.: Application of the Method of Characteristics to Noncircular Bodies at Angle of Attack. Analytic Methods in Aircraft Aerodynamics, NASA SP-228, 1969, pp. 159-176.
10. Kutler, Paul, and Lomax, Harvard: A Systematic Development of the Supersonic Flow Fields Over and Behind Wings and Wing-Body Configurations Using a Shock-Capturing Finite-Difference Approach. AIAA Paper No. 71-99, Jan. 1971.
11. Kirkham, F. S.; and Driver, C.: Energy Supply and Its Effect on Aircraft of the Future. Part II: Liquid-Hydrogen-Fueled Aircraft - Prospects and Design Issues. AIAA Paper No. 73-809, Aug. 1973.
12. Anderson, Griffin Y.: An Examination of Injector/Combustor Design Effects on Scramjet Performance. NASA paper presented at the 2nd International Symposium on Air Breathing Engines (Sheffield, England), Mar. 25-29, 1974.
13. Henry, John R.; and Anderson, Griffin Y.: Design Considerations for the Airframe-Integrated Scramjet. NASA TM X-2895, 1973.

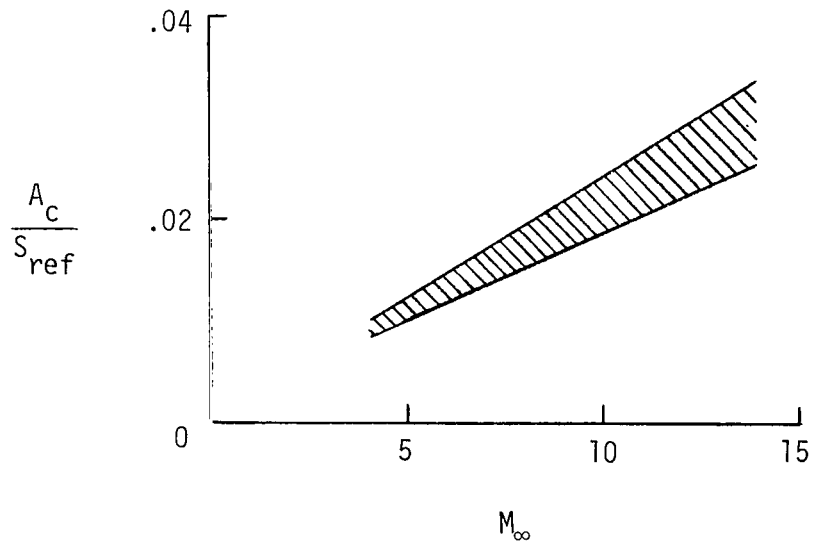
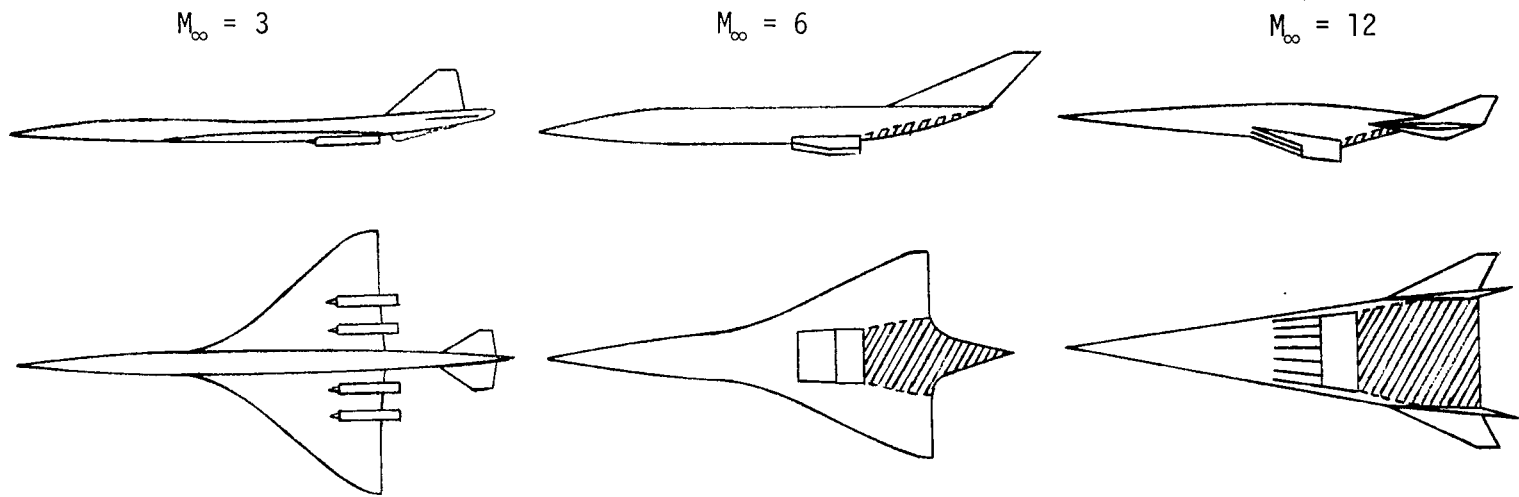


Figure 1.- Required inlet capture.

DESIGN FOREBODY TO MEET AERODYNAMIC,  
ENGINE INLET, AND VEHICLE VOLUMETRIC  
REQUIREMENTS.

DESIGN NOZZLE-AFTBODY  
FOR THRUST, STABILITY,  
AND LOW TRIM DRAG.

SIZE SCRAMJETS TO MEET  
MISSION REQUIREMENTS.

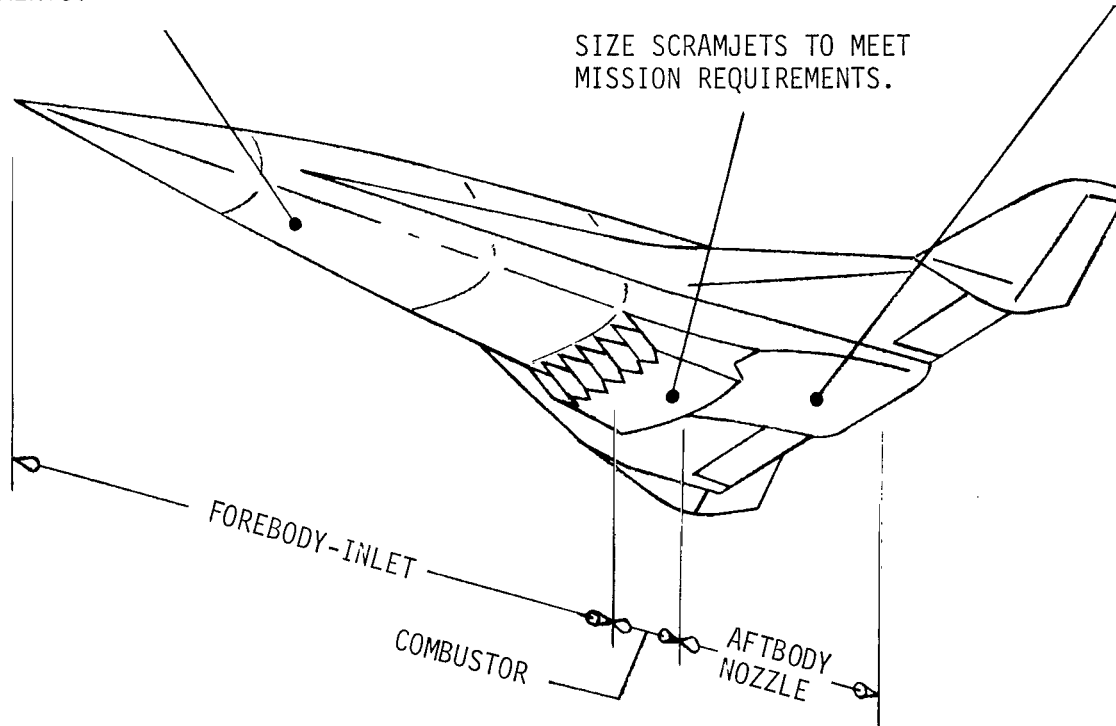


Figure 2.- Design features for efficient engine airframe integration.

DESIGN GOALS

MINIMIZE INLET FLOW GRADIENTS.

MASS FLOW  
PRESSURE  
LOCAL MACH NUMBER

MINIMIZE SENSITIVITY WITH MACH  
NUMBER AND ANGLE OF ATTACK.

MAXIMIZE EFFECTIVE INLET CAPTURE.

MAINTAIN UNIFORM BOW SHOCK  
STAND-OFF DISTANCE

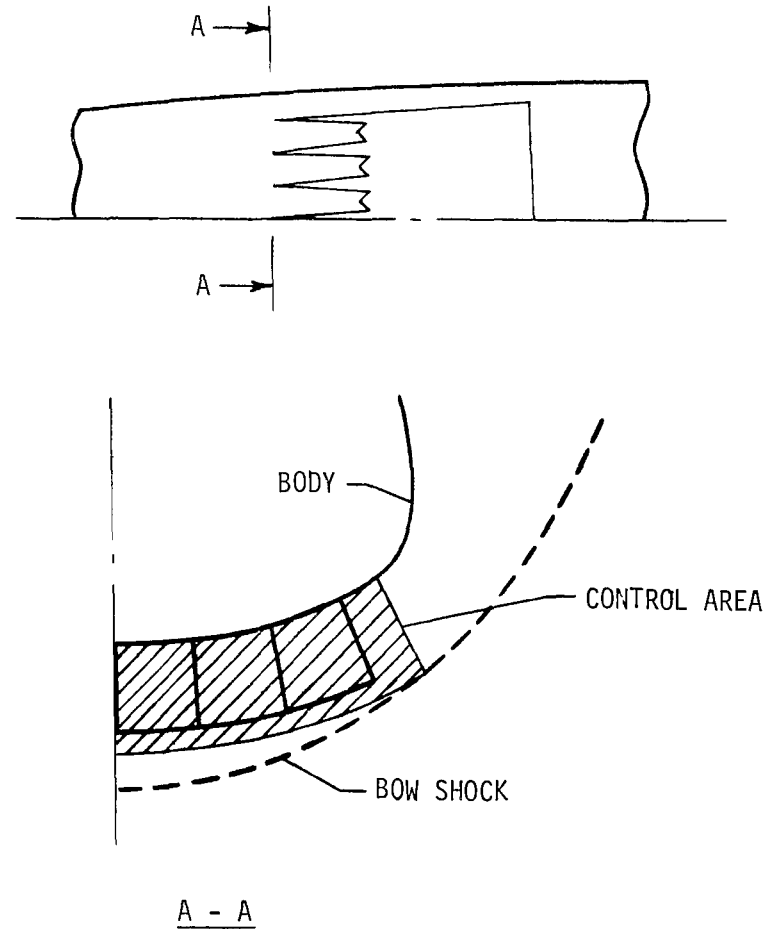
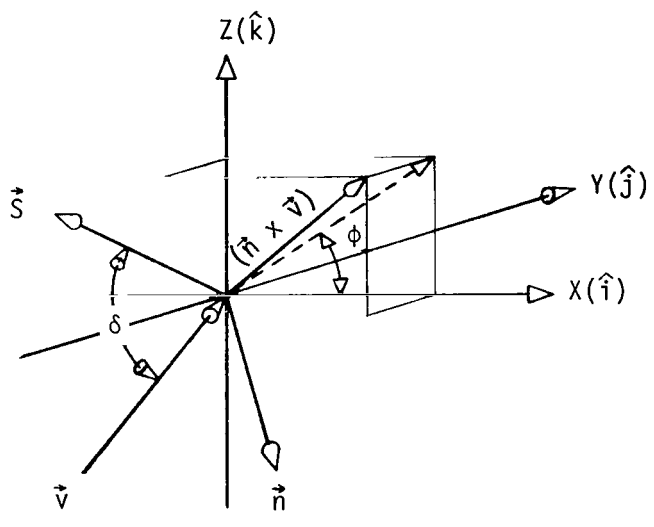
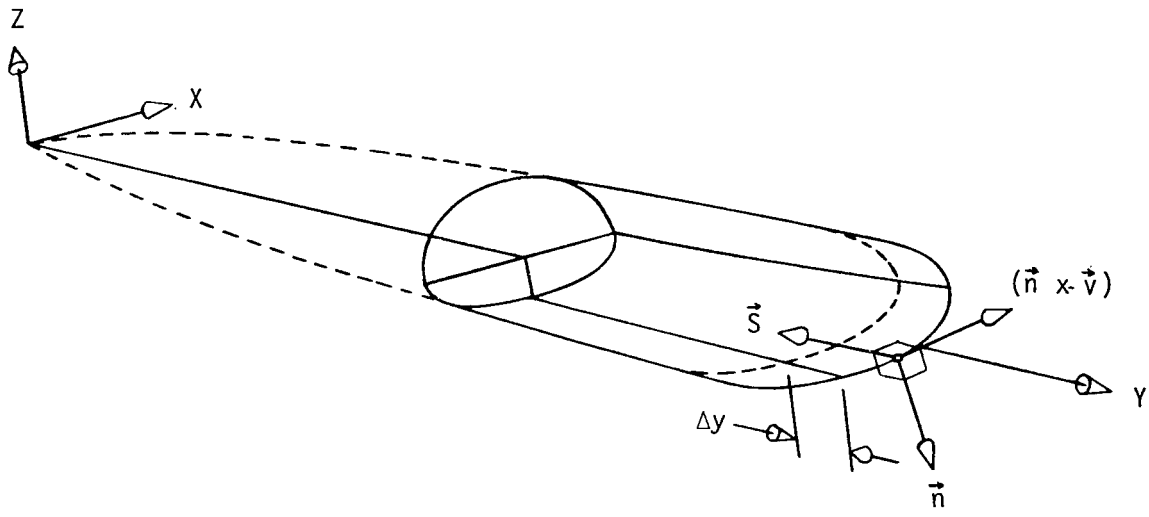


Figure 3.- Forebody design goals.



SKETCH OF LOCAL VECTOR DIRECTIONS

Figure 4.- Relation between body geometry and wind vector for Newtonian impact angle.

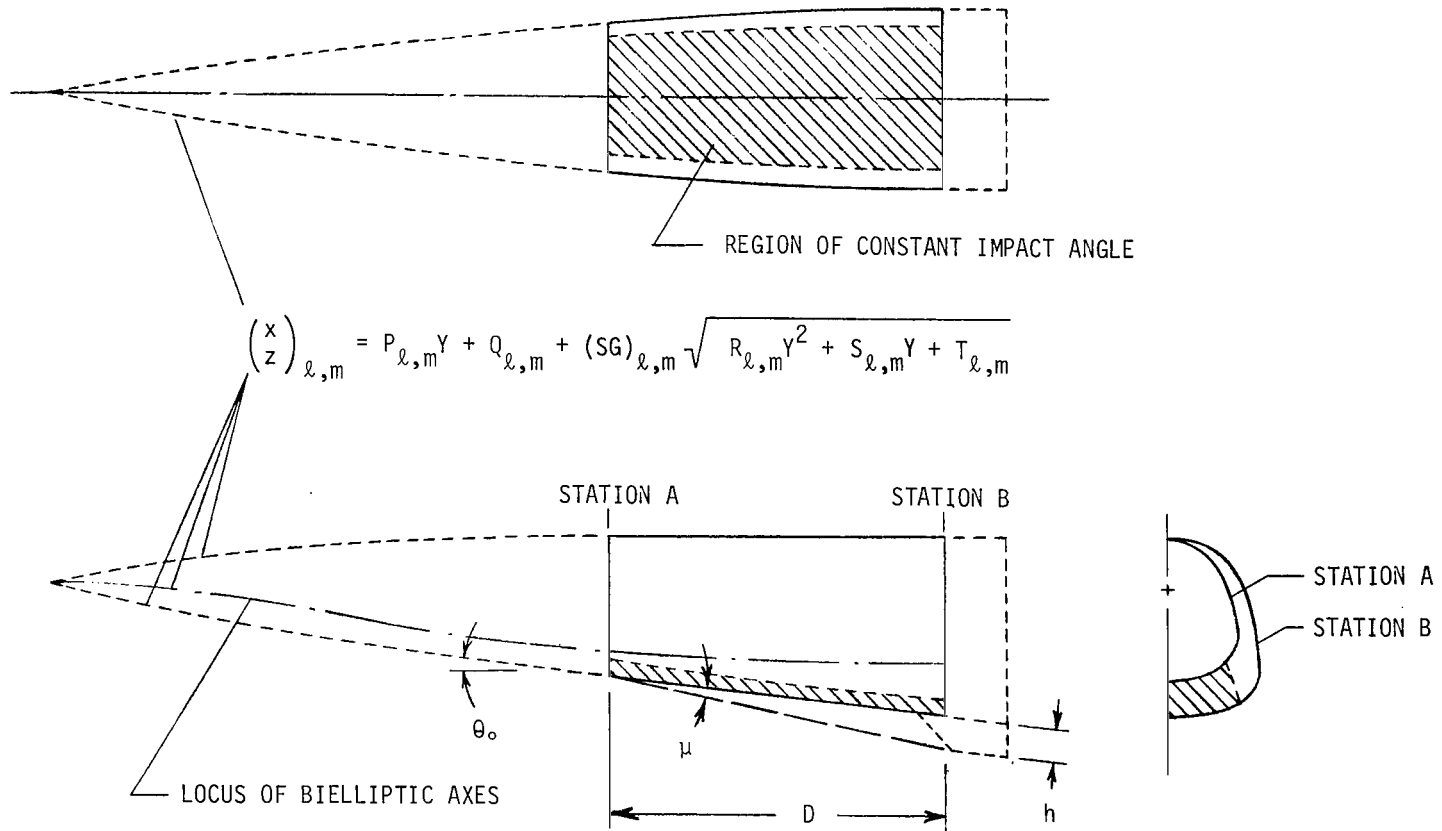


Figure 5.- Geometry definition for bielliptic forebody design.

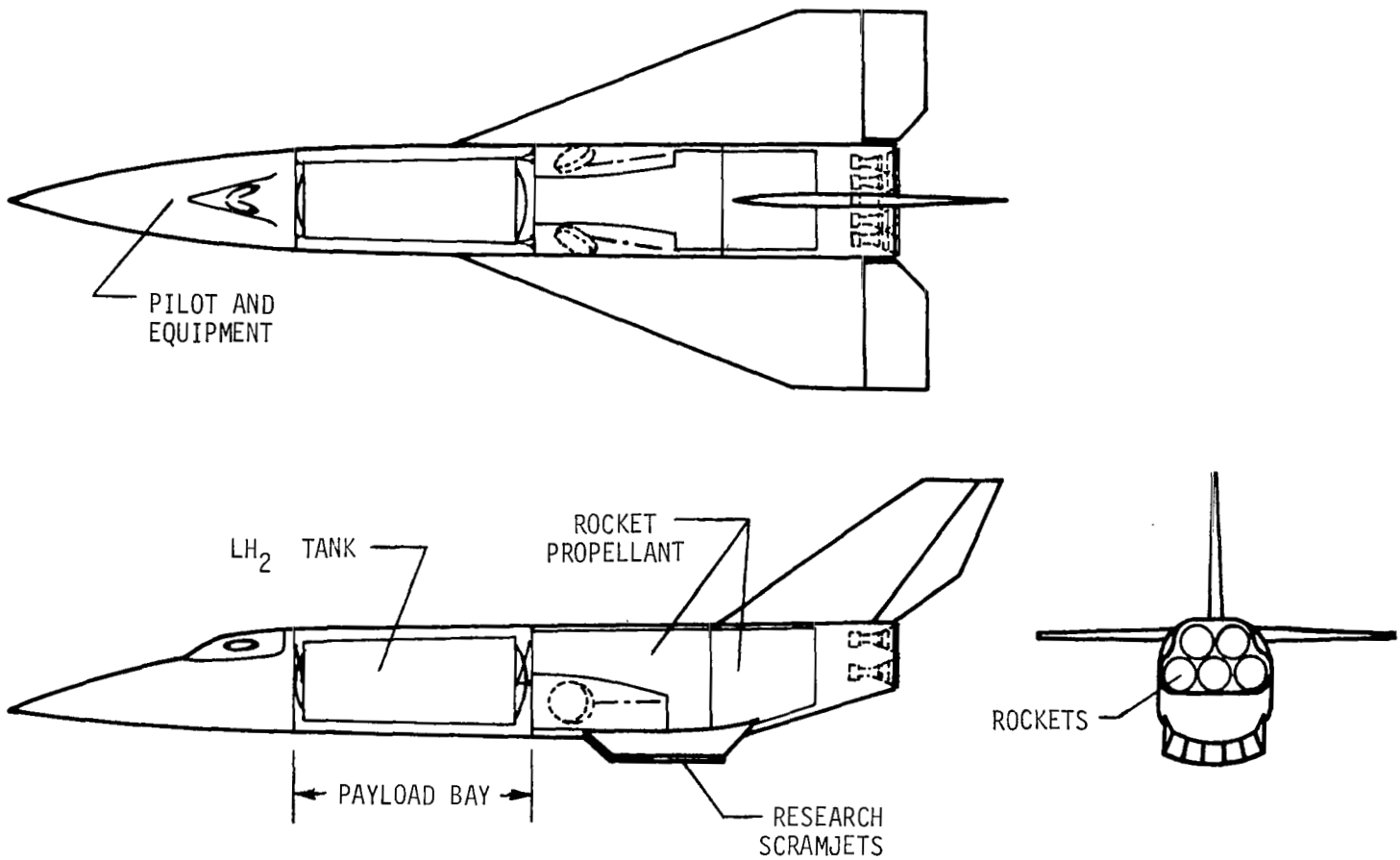


Figure 6.- Basic elements of high-speed research airplane (HSRA).

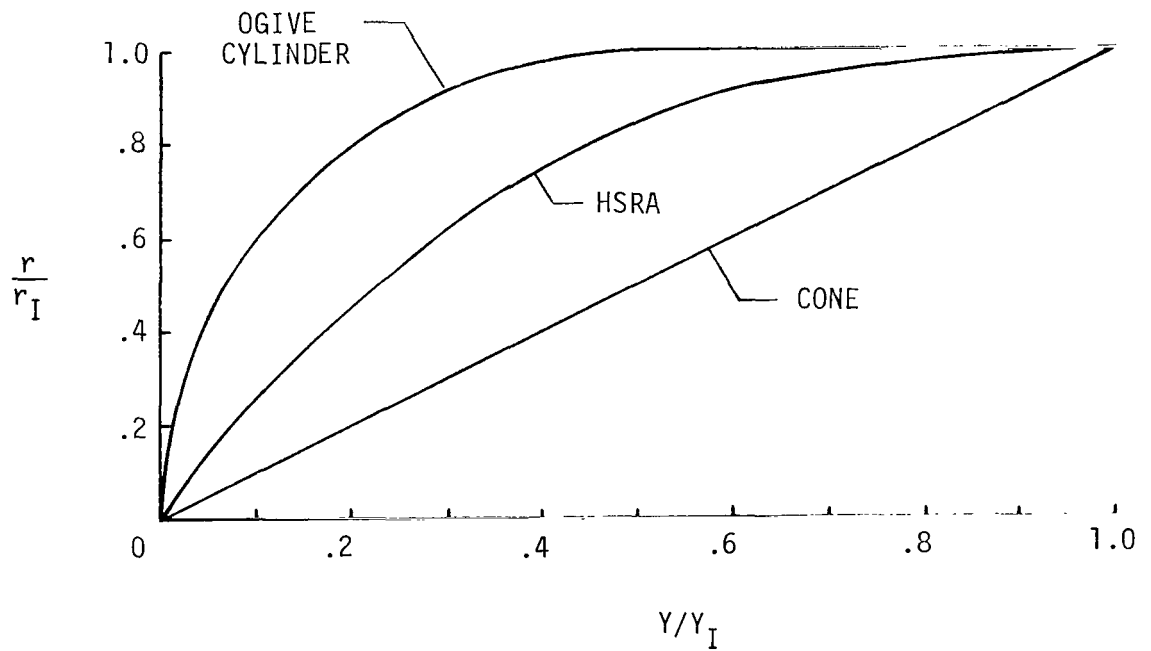
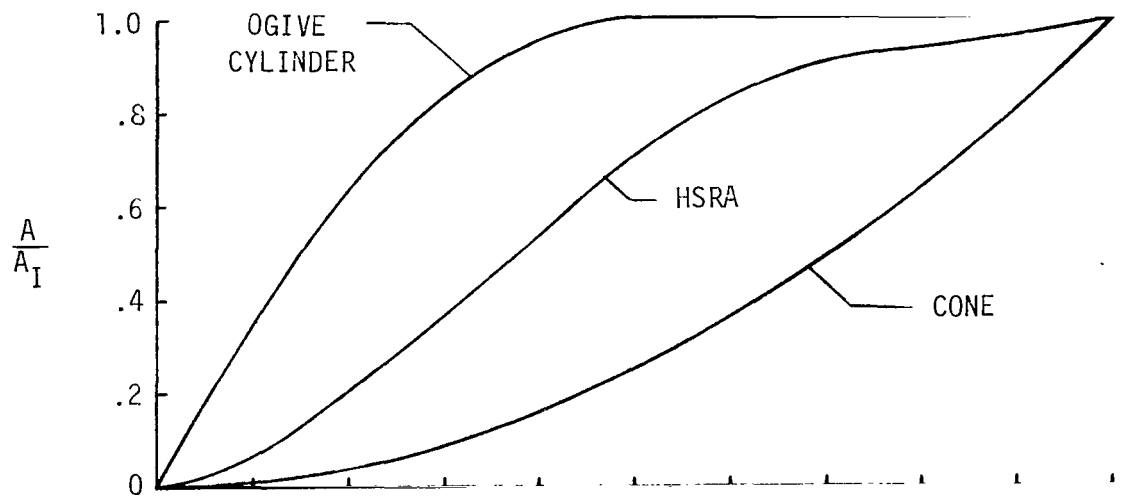


Figure 7.- Volumetric requirements of high-speed research airplane (HSRA) forebody.

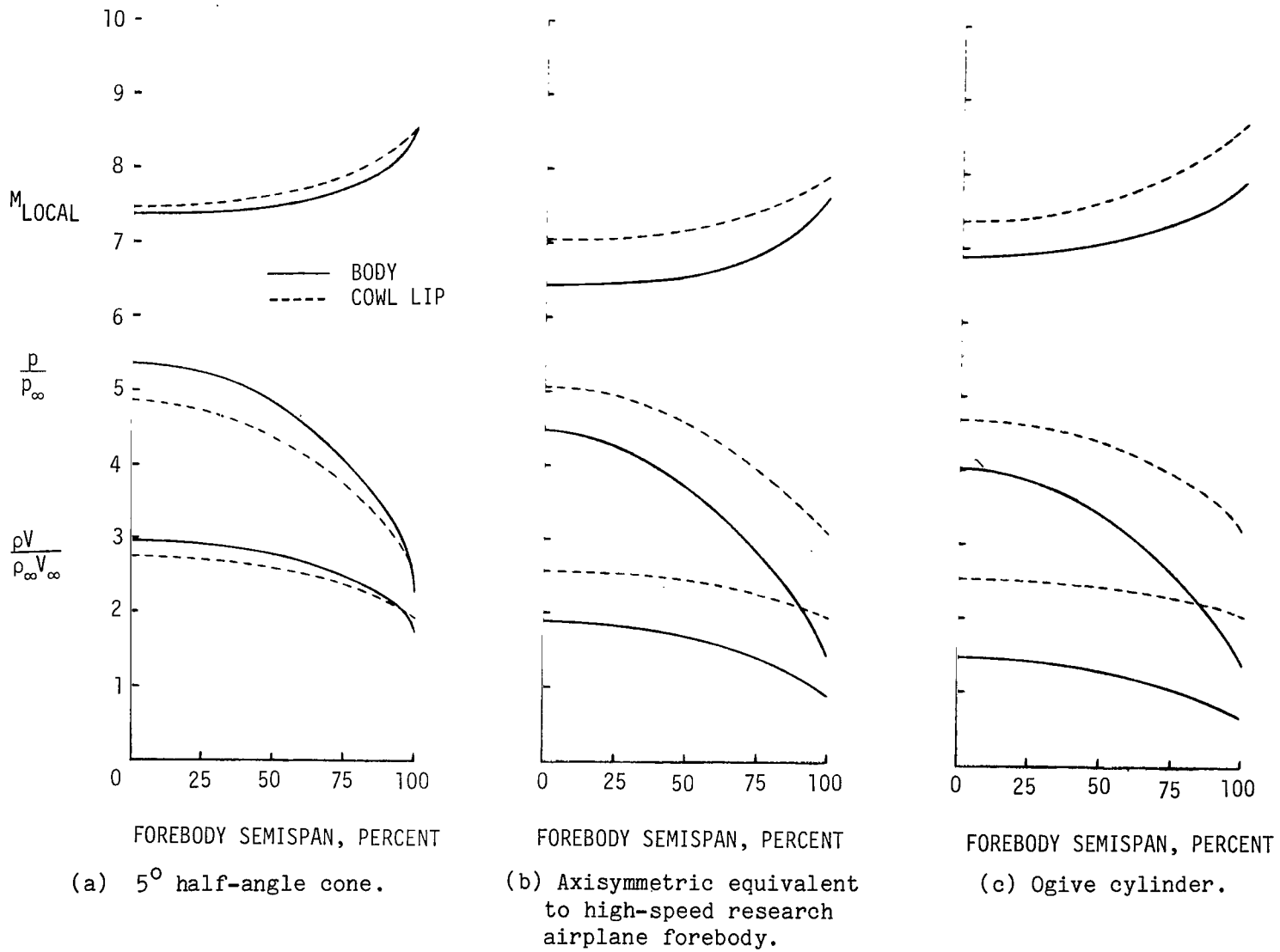


Figure 8.- Comparison of flow at inlet entrance generated by axisymmetric alternatives to high-speed research airplane forebody;  $M_{\infty} = 10$ ,  $\alpha = 10^{\circ}$ .

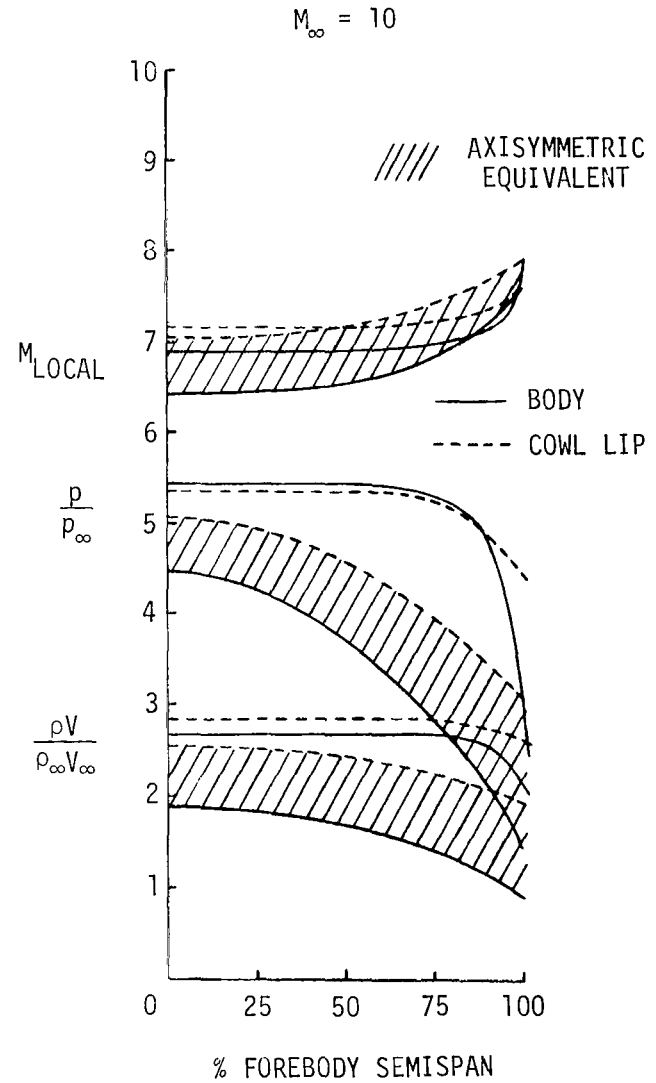
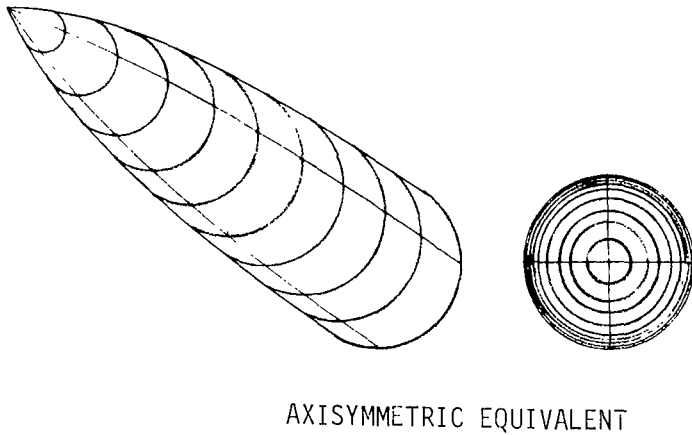
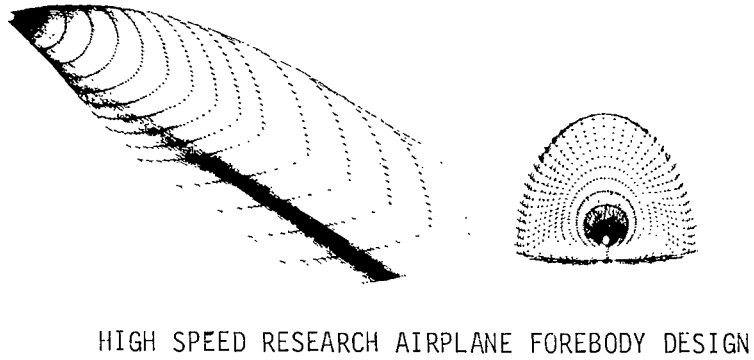


Figure 9.- Comparison of inlet entrance flow conditions between constant Newtonian impact-angle forebody and its axisymmetric equivalent.

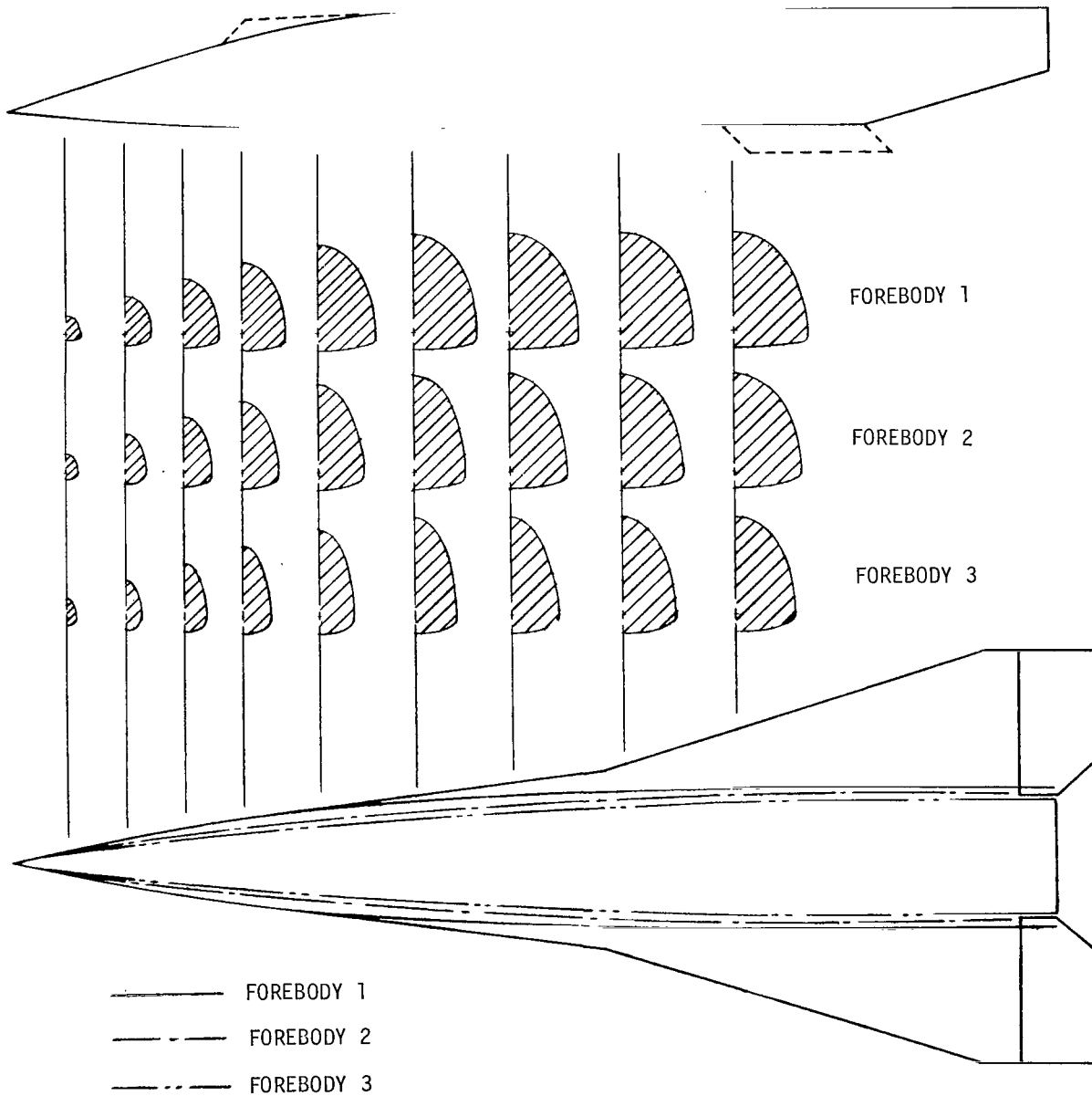


Figure 10.- Forebody designs producing uniform precompressed flow at inlet entrance.

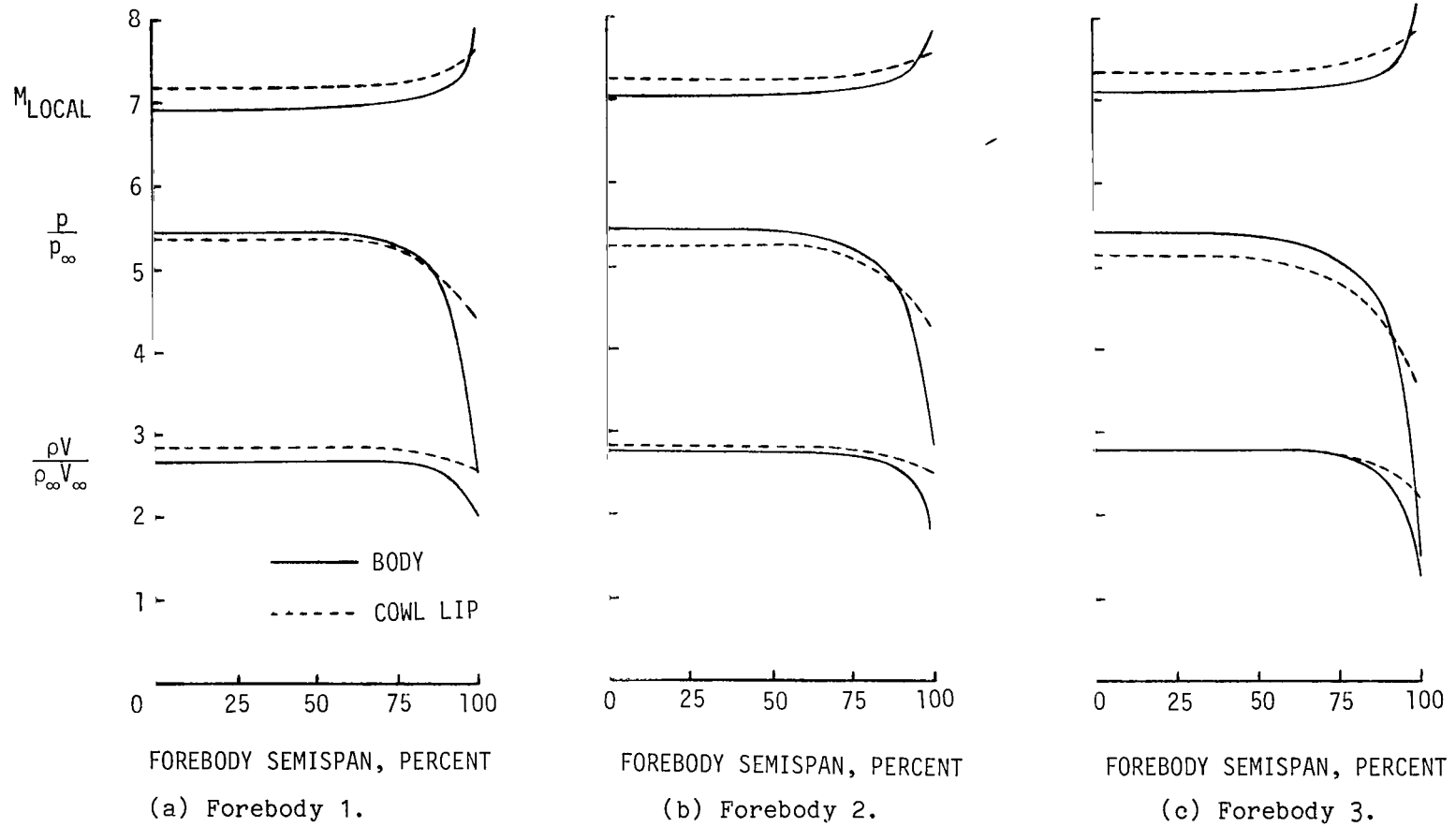


Figure 11.- Flow conditions at inlet for three forebody designs at  $M_{\infty} = 10$  and  $\alpha = 10^{\circ}$ .

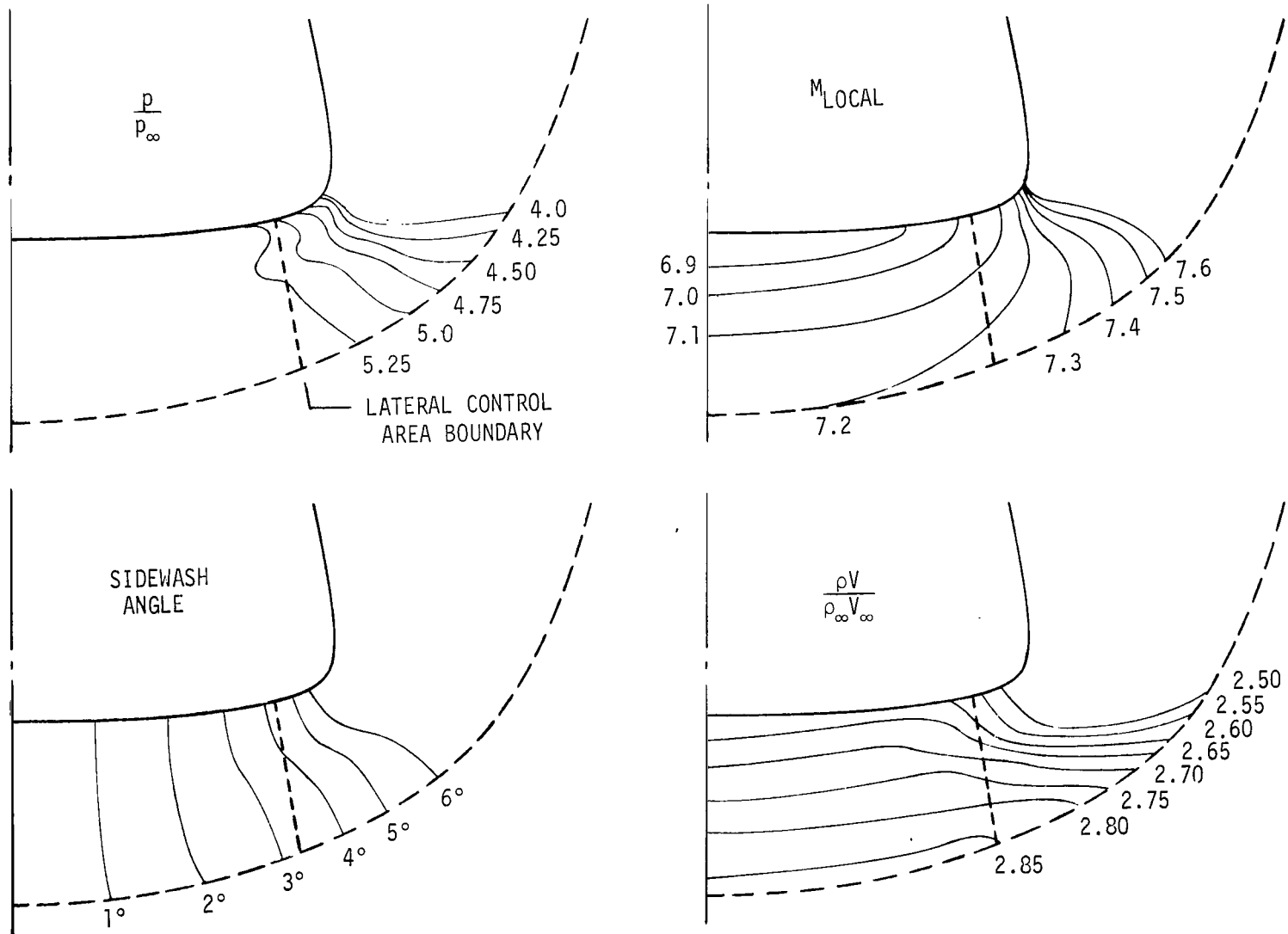


Figure 12.- Flow isograms at inlet entrance produced by forebody 1 at  $M_\infty = 10$  and  $\alpha = 10^\circ$ .

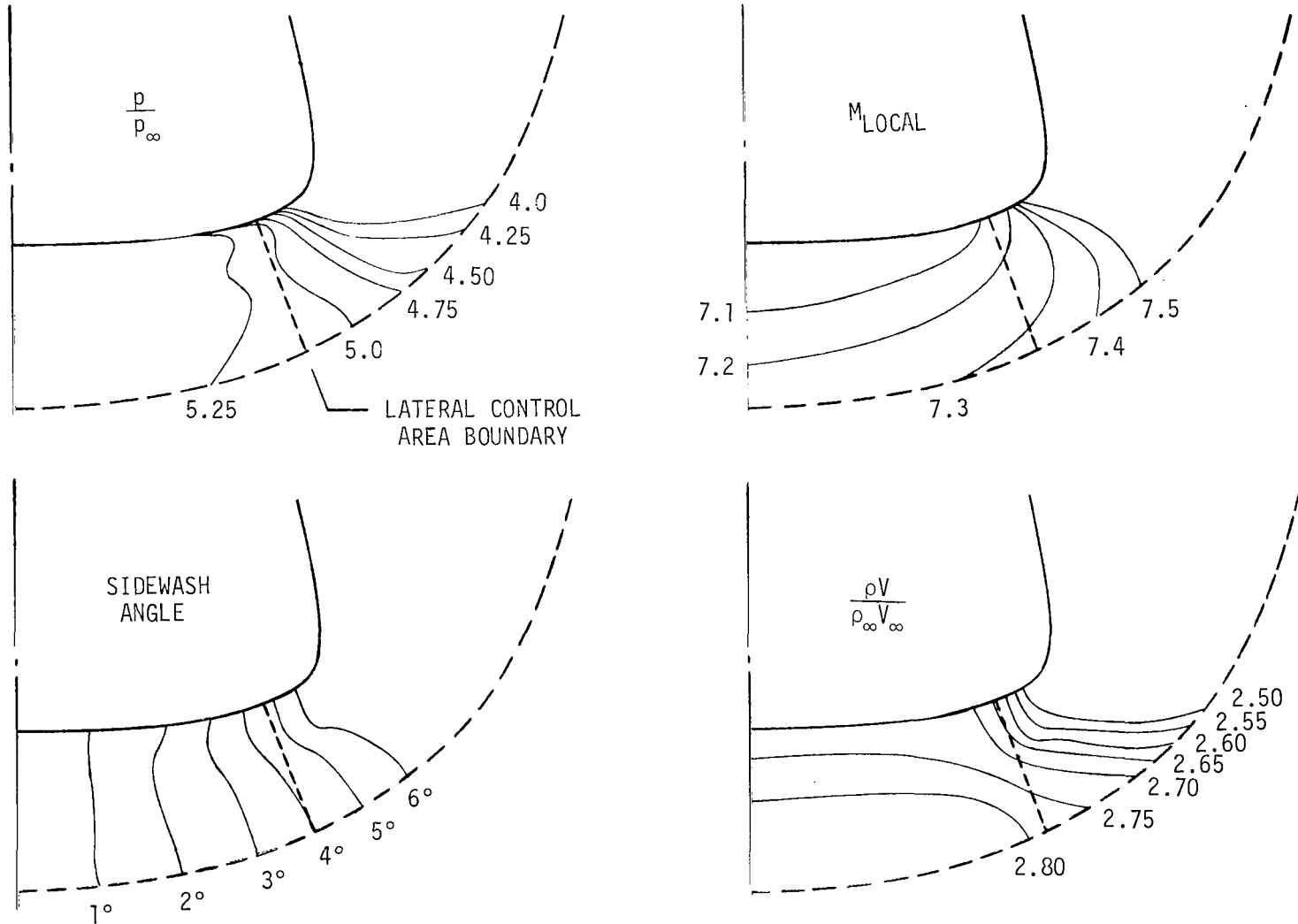


Figure 13.- Flow isograms at inlet entrance produced by forebody 2 at  $M_\infty = 10$  and  $\alpha = 10^\circ$ .

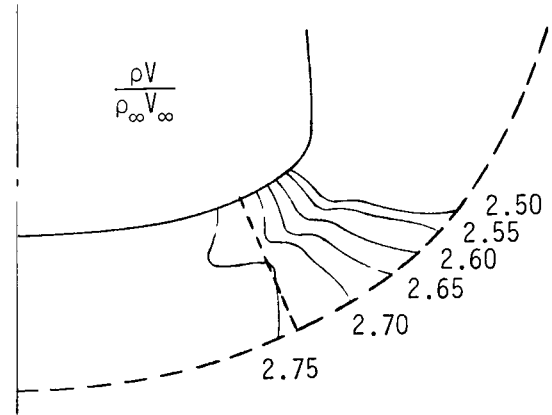
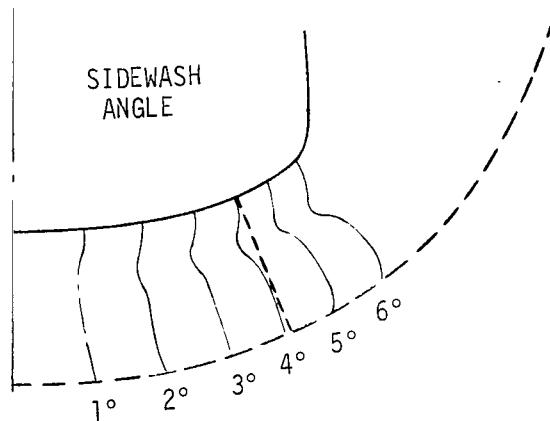
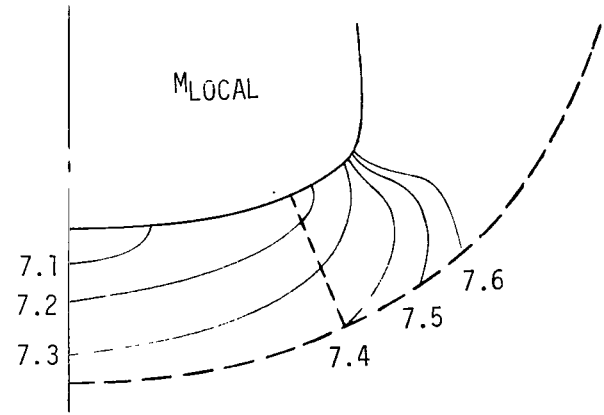
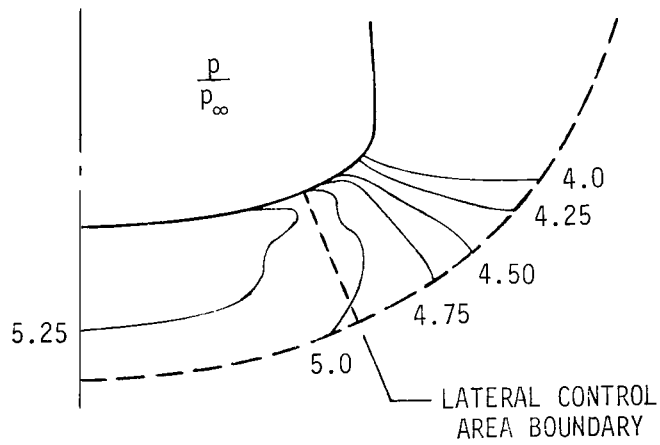


Figure 14.- Flow isograms at inlet entrance produced by forebody 3 at  $M_\infty = 10$  and  $\alpha = 10^\circ$ .

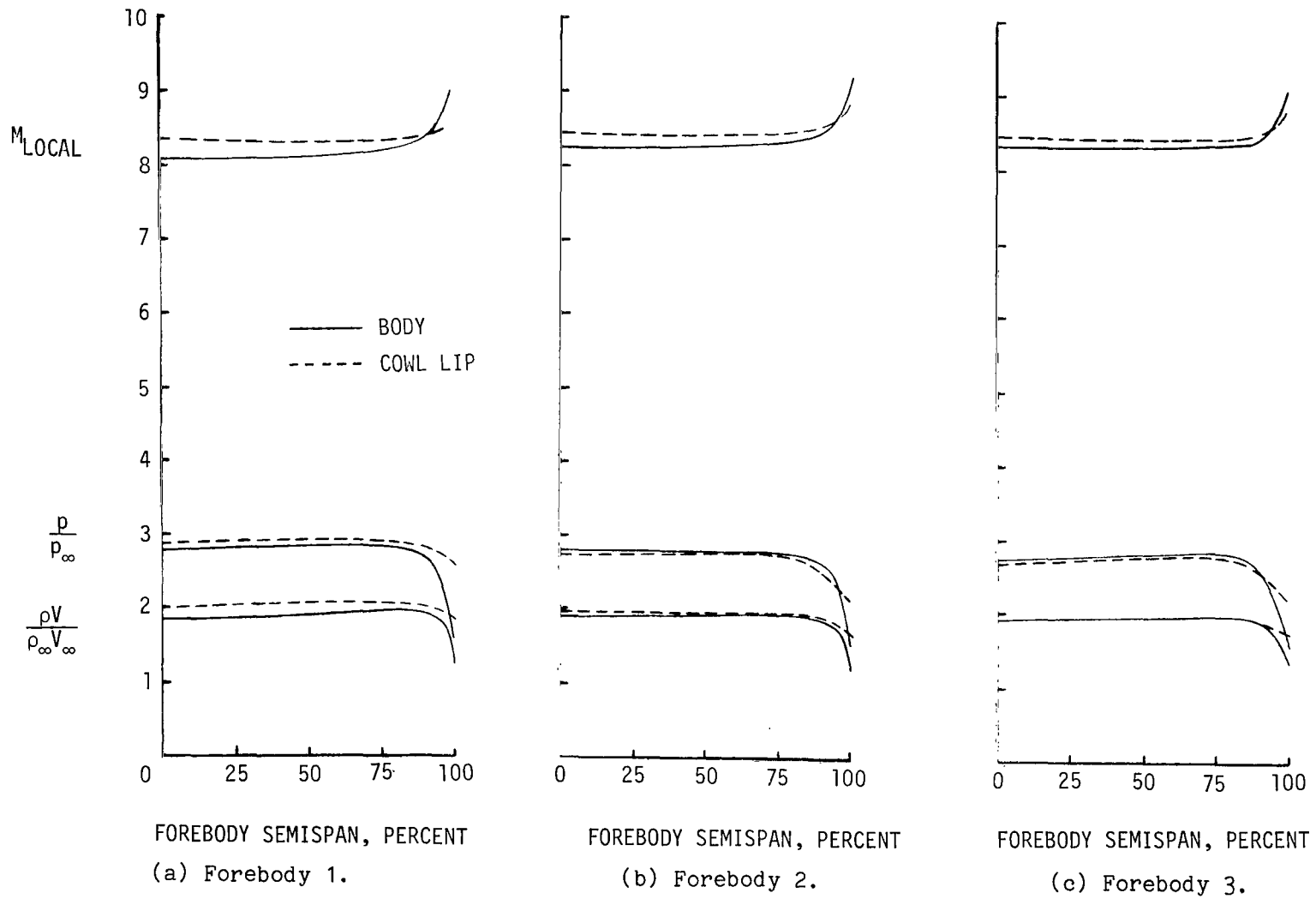


Figure 15.- Inlet entrance flow conditions corresponding to acceleration angle of attack ( $\alpha = 6^\circ$ ) at  $M_\infty = 10$ .

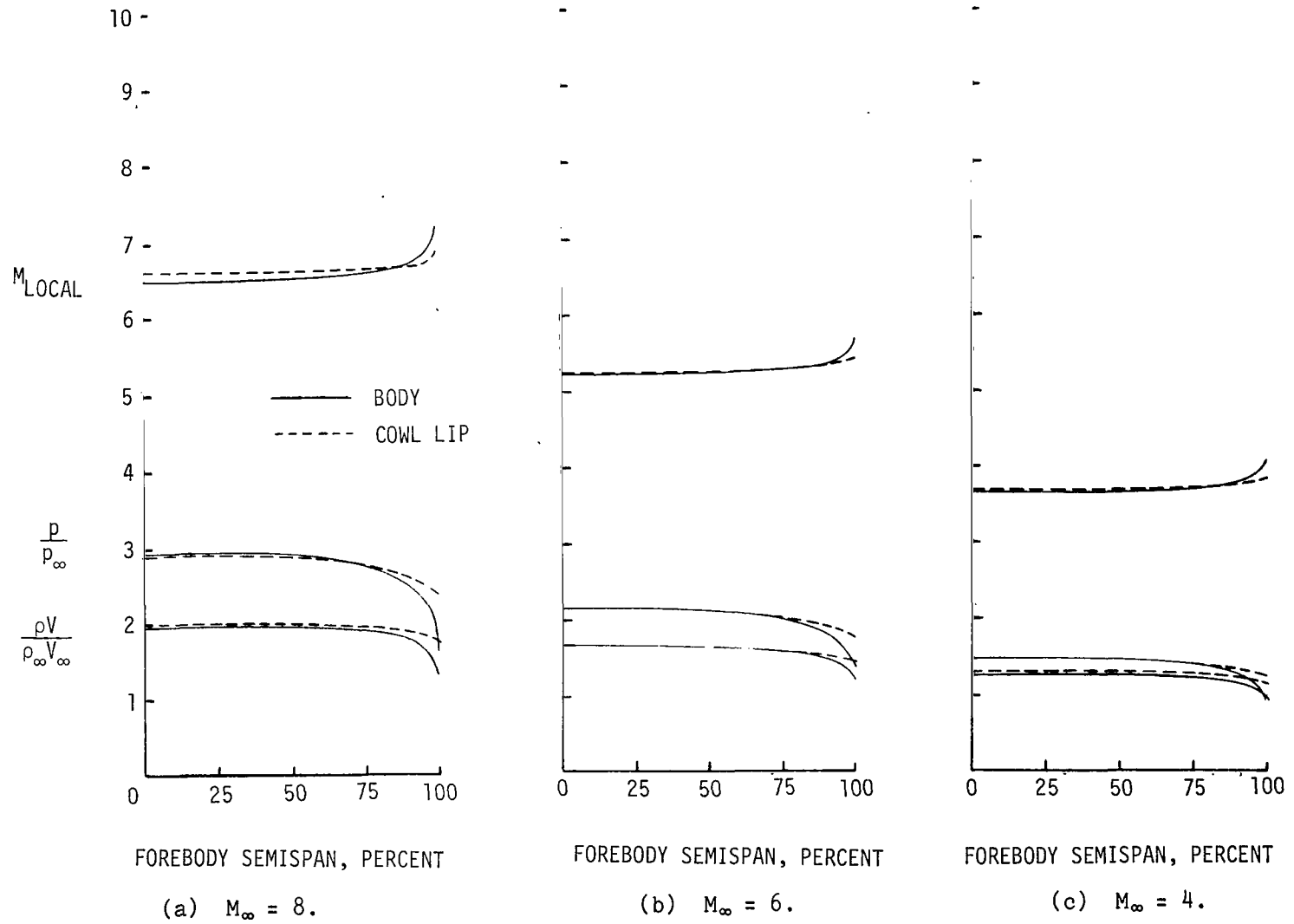


Figure 16.- Off-design flow at inlet entrance produced by forebody 1 at acceleration angle of attack ( $\alpha = 6^\circ$ ).



059 001 C1 U A 770114 S00903DS  
DEPT OF THE AIR FORCE  
AF WEAPONS LABORATORY  
ATTN: TECHNICAL LIBRARY (SUL)  
KIRTLAND AFB NM 87117

MASTER : If Undeliverable (Section 158  
Postal Manual) Do Not Return

*"The aeronautical and space activities of the United States shall be conducted so as to contribute . . . to the expansion of human knowledge of phenomena in the atmosphere and space. The Administration shall provide for the widest practicable and appropriate dissemination of information concerning its activities and the results thereof."*

—NATIONAL AERONAUTICS AND SPACE ACT OF 1958

## NASA SCIENTIFIC AND TECHNICAL PUBLICATIONS

**TECHNICAL REPORTS:** Scientific and technical information considered important, complete, and a lasting contribution to existing knowledge.

**TECHNICAL NOTES:** Information less broad in scope but nevertheless of importance as a contribution to existing knowledge.

**TECHNICAL MEMORANDUMS:** Information receiving limited distribution because of preliminary data, security classification, or other reasons. Also includes conference proceedings with either limited or unlimited distribution.

**CONTRACTOR REPORTS:** Scientific and technical information generated under a NASA contract or grant and considered an important contribution to existing knowledge.

**TECHNICAL TRANSLATIONS:** Information published in a foreign language considered to merit NASA distribution in English.

**SPECIAL PUBLICATIONS:** Information derived from or of value to NASA activities. Publications include final reports of major projects, monographs, data compilations, handbooks, sourcebooks, and special bibliographies.

**TECHNOLOGY UTILIZATION PUBLICATIONS:** Information on technology used by NASA that may be of particular interest in commercial and other non-aerospace applications. Publications include Tech Briefs, Technology Utilization Reports and Technology Surveys.

*Details on the availability of these publications may be obtained from:*

**SCIENTIFIC AND TECHNICAL INFORMATION OFFICE**

**NATIONAL AERONAUTICS AND SPACE ADMINISTRATION**

**Washington, D.C. 20546**